(2)

Penn State

A Study of the Gas Phase Chemistry of Solid Propellants Using a Microprobe Mass Spectrometer (MPMS) System

Second Annual Report

Preliminary Results for Solid Fuels (HTPB/Zecorez and BAMO/NMMO), Single-Base Propellant (M10) and an RDX-Based Propellant (BLX-9)

Thomas A. Litzinger

ONR Grant No. N00014-89-J-1238
under supervision of Dr. R.S. Miller

~~1990~~ 1991

TABLE OF CONTENTS

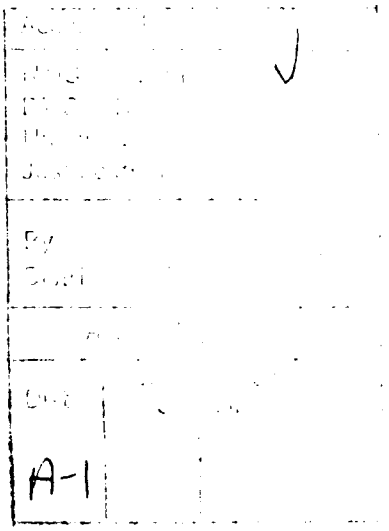

1.0 INTRODUCTION

Detailed knowledge of the gas-phase reactions which occur during propellant ignition and combustion are required to understand and model these processes. If detailed models were available, modification of propellant formulations for improved combustion behavior could be achieved with much less trial-and-error testing. Furthermore, detailed models could be used to generate simplified kinetics schemes for use in propellant models. Without a firm basis for these simplified kinetic schemes, the kinetic parameters are often adjusted to fit burning rate and ignition data; thus, the propellant models are reduced to sophisticated curve fits to experimental data. Clearly, knowledge of the gas-phase chemistry during propellant ignition and combustion has practical consequences.

The significance of gas-phase reactions in propellant ignition and combustion is highlighted by a series of special workshops on gas-phase reactions related to propellants which began at the 24th JANNAF Combustion Meeting in 1987. At these meetings, the state of the art in the modelling, kinetics and diagnostics related to propellant ignition and combustion are discussed by experts in these fields. A recurring theme during the first workshop was the need to understand the behavior of individual ingredients of propellants as a first step towards understanding the complete interactions which occur in real propellants. Discussions also pointed to the need for the most basic information such as the thermal structure in the gas-phase and the surface temperature. Also, the need to acquire species concentration profiles in the gas-phase was identified as critical to the advancement of the field.

The present research program, designed to address this critical shortage of gas-phase data for propellant ingredients of significance to the Navy, centers around the development and application of a microprobe, mass spectrometer (MPMS) system to study the gas phase chemistry of solid propellant ingredients and solid propellants during heating by a CO_2 laser and during steady combustion. The MPMS system uses quartz microprobes with orifice sizes of 100μm or less to withdraw gases from the region above the sample material. Through a two stage pumping system, the sample is delivered to a quadrupole mass spectrometer for analysis. Sampling is continuous throughout the combustion event so that species profiles of stable intermediates above the sample are obtained during the experiments. In addition to the MPMS system, existing experimental methods to be used in the work include high speed direct photography, high speed schlieren photography, microthermocouple probes and photodiodes (for first visible light).

During the second year of this program, several key improvements were made in the MPMS system that improved its temporal response and spatial resolution. These modifications are discussed in the first section of the report. Also, testing was begun with a variety of materials including HTPB/Zecorez, BAMO/NMMO, M10 (a single base nitrocellulose propellant) and BLX-9 (an RDX-based material). The results of these tests are summarized in the second section of this report. Of

particular note are the BLX-9 results which quite clearly show the various zones associated with nitramine propellants. These results indicate that the MPMS system can resolve the structure of nitramine flames at atmospheric pressure.

2.0 MPMS SYSTEM ENHANCEMENT

Several significant improvements were made to the MPMS system in the second year of operation. A Keithley current amplifier and a Hewlett Packard programmable universal source were added to the electronics system to enhance system performance (see Figure 1). Changes in the primary microprobe size, geometry, and method of construction and in the positioning of the secondary microprobe greatly enhanced the performance and resolution of the gas sampling system. It was discovered that angling the sample surface toward the microprobe also enhanced the efficiency of gas sampling under laser heating. The mass spectrometer unit (MSU) and microprobe axial alignment were greatly improved using precise centering techniques.

2.1 Keithley Preamplifier

A Keithley 427 analog current amplifier was added to the MPMS system electronics, replacing the preamp supplied with the Extrel EX500 system. The Keithley preamp greatly enhanced the electronic speed of the system, improved the signal-to-noise ratio, and allowed greater freedom in choosing the optimum gain setting for amplifying the multiplier output signal. The preamp control panel provides for manual control of the signal rise time (determined by 10%-90% signal rise) with a minimum setting of 0.01 ms. For most of the experimental runs, a setting of 0.1 ms has been employed which optimizes the signal-to-noise ratio for low concentration species without affecting system speed or sensitivity. The manual gain adjustment has eight settings from 10^4 to 10^{11} signal amplification as opposed to the three settings with the original preamp that were set with the sensitivity control on the electrometer module. As indicated in Figure 1, all manual signal modification controls on the electrometer module are now bypassed. The signal is modified only with the preamp controls and then sent directly to the monitor for display or to the computer for recording and processing.

2.2 Hewlett Packard Universal Source

A Hewlett Packard programmable universal source, model HP 3245A, was added to the MPMS control electronics for more precise control of the MSU and for increased flexibility in selecting the specific amu or amu range to be sampled during the test event. The HP 3245A generates precise DC voltage outputs from -10 to +10 VDC with 6 digits of resolution (24 bits) in high resolution mode. It can be programmed to generate arbitrary waveforms up to 1 MHz or ramp waveforms up to 100 KHz. The source has selectable input trigger sources/events and can also deliver output trigger signals. The Mass Spectrometer Control and Data Acquisition program is currently being modified to incorporate the HP universal source as the controlling signal input to the mass spectrometer.

2.3 Gas Sampling System Enhancements

The efficiency and resolution of the gas sampling system were greatly enhanced through numerous modifications to both microprobes and by angling the propellant sample surface toward the microprobe. Figure 2 shows the gas sampling setup from the primary microprobe entrance to the

ionizer entrance. The major changes depicted here include the use of smaller 3.2 mm O.D. primary microprobes, angling of the sample surface, use of a primary probe shield to protect the probe from laser-induced heating, and changes in the positioning and the length of the secondary microprobe. A better vacuum seal for both microprobes was obtained by installing CAJON Ultra-Torr fittings that use O-ring seals, replacing the orignal Swagelok fittings that used Teflon ferrules for sealing. Both CAJON fittings were bored through so that the microprobes could be slid through the fittings, allowing flexibility in positioning.

2.3.1 Primary Microprobe

The primary microprobe tube size was reduced to 2 mm I.D. by 3.2 mm O.D from the original 3.2 mm I.D. by 6.4 mm O.D. tube size. The reduction in external tube diameter considerably reduced the inherently intrusive nature of the microprobe sampling. This can be seen in the photograph in Figure 3 which compares the two microprobe sizes in relation to a propellant sample. High-speed schlieren video movies of the gas flow around the probes also gave evidence of the reduction in flow disturbance by using the smaller primary microprobes.

2.3.2 Sample Surface Geometry

Small adapters were constructed and installed on the sample holder to angle the sample surface toward the microprobe at angles from 30° to 45°. Problems were encountered when a flat sample surface was used due to the vertically incident laser beam being partially blocked by the probe. The sample surface generating the sampled gases was right on the blocked/irradiated dividing line and the surface in this region often burned unevenly due to beam diffraction and radial heat conduction. This caused ambiguity in measuring the surface to probe orifice sampling height. By angling the sample, the surface generating the sampled gases was shifted from the vertical axis so that it was unaffected by the probe/beam interactions and burned uniformly throughout the test. High-speed schlieren photography showed that over the sampling distances employed in generating the species profiles, no upward deflection of the gas flow streamlines normal to the surface due to free convection effects was evident. Another advantage of angling the sample surface was that, with the surface angle being greater than the half angle of the probe tip (≈15°), the probe tip could be initially positioned right on the sample surface. This produced an initial sampling height equal to half the probe tip diameter times the cosine of the surface angle, which is ≈100 μm with the current setup.

2.3.3 Secondary Microprobe

Secondary microprobe modifications included positioning of the secondary microprobe orifice right at the exit of the primary microprobe and lengthening the probe so that its exit was about 0.61 cm from the ionizer entrance. A centering fixture was fabricated from 0.64 mm copper sheet with a rubber grommet installed to support the microprobe (see Figure 2). The fixture was designed to slide into the primary chamber tube nearest the primary microprobe so that the probes axes would be

precisely aligned. The front flange containing the primary microprobe was chamfered at an angle slightly larger than the secondary probe half angle to allow that probe to be positioned right at the exit of the primary probe. This positioning enhanced the sampling efficiency of the secondary microprobe, improving the signal strength and the signal-to-noise ratio by reducing the amount of background gases that could be entrained in the sample gas 'beam.' The primary-to-secondary probe clearance was set with the vacuum system in operation by sliding the primary probe back in its fitting until it was positioned as close as possible to the secondary probe without causing restriction of the flow through the primary probe into the primary chamber. Blockage of this flow was observed by a decrease in the primary chamber pressure and an increase in the quadrupole chamber pressure.

Also depicted in Figure 2 is a beam shield made of 0.64 mm thick copper sheet, which has a reflectivity of about 97% at the laser's wavelength of 10.6 μm. Preliminary tests showed that with relatively high laser beam intensity and/or long duration of laser heating, the microprobe tip would glow red hot due to the radiative heating and the shield was constructed to alleviate this problem.

2.3.4 Microprobe Construction

A major improvement in the microprobe sampling resulted from changes in the method of developing the final probe shape and sampling orifice size. A new method of probe construction allowed the probes to be finished to finer dimensions both in external size, again reducing the intrusiveness, and in sampling orifice size, which greatly enhanced the spatial resolution of the sampling system. As was described in the first annual report, a small region of the quartz tubing was heated while it was spun in a lathe and the tubing was pulled until two conical tips formed in this heated area. The tube was then cut in half at the tip of the cones, leaving two blank (i.e., no orifice) microprobes. Originally, the conical probe nose was then ground down on a diamond wheel and the tip was faced off to obtain an orifice. Due to the roughness of the diamond wheel, the external surface of the probe could not be finished very smoothly or made to fine dimensions. Also, the orifice size could not be made to the desired small sizes (d≈25 μm) and the sizing was quite arbitrary.

To alleviate these limitations, the blank probes were finished with manual sanding using a special setup. 220 and 400 grit sandpaper were used to rough finish the probes and 600 grit sandpaper was used to polish the final external surface and to carefully sand back the face of the probe tip until the desired sampling orifice size was obtained. All operations were carefully monitored under a 12X illuminated aspheric magnifier from Edmund Scientific Co. However, even with the magnifier, the desired sampling orifice sizes of 15-30 μm were difficult to see, not only due to the small size but also due to the possibility of sanding grit blocking the hole. To efficiently attain these small orifice sizes, final sanding of the tip with the 600 grit sandpaper was performed in a small, shallow dish of water with air pressure of about 20 psig applied to the back of the probe through a Tygon tube. As soon as the blank probe tip face was sanded through and an orifice

developed, tiny air bubbles were observed in the water bath. The air flow kept the orifice free of debris and, with experience, the size and amount of the air bubbles became a strong initial indicator of probe orifice size. The actual orifice size was measured under a microscope.

The new method of probe construction also made it easier to create probes with smaller external dimensions since the probe wall thickness could be slowly sanded away and the thickness could be accurately monitored under the illuminated magnifier. The finished probes could thus be made more streamlined and obviously less intrusive. Also, the probe tip face diameter could be made smaller and measured quite accurately. As was mentioned earlier, angling the sample surface permitted the probe to be positioned right on the surface with the initial sampling height determined by the probe tip diameter. Therefore, reducing the tip diameter also reduced the minimum initial sampling height so that the important species profiles very close to the sample surface could be measured more precisely.

3.0 PRELIMINARY RESULTS

Preliminary results for tests of several different materials will be discussed in this section. The data presented include identification of molecular weights of major and minor species, temporal species profiles, and spatial species profiles. The materials tested and discussed here include two solid fuels and two propellants. One of the main priorities of these tests was to develop and improve the procedures coordinating the experimental control with the multiple forms of data acquisition. Therefore tests were run with various forms of data acquisition being performed in different combinations.

3.1 Solid Fuels

The solid fuels tested were an HTPB/Zecorez composition and the energetic copolymer BAMO/NMMO. The first checkout tests of the MPMS system were performed with BAMO/NMMO samples, and these initial results will be discussed briefly. Several tests of HTPB/Zecorez were conducted after the major MPMS system modifications had been implemented. Two different testing methods were attempted both to study the HTPB/Zecorez material and to ascertain the system's temporal resolution.

3.1.1 BAMO/NMMO

Only analysis of post-test species wad performed for the copolymer BAMO/NMMO; species profiles were not obtained. Pyrolysis tests were conducted in a helium environment at one atmosphere with a heat flux of 225 W/cm^2 for two seconds. The major species identified were H_2O, H_2, and several possible species at producing a major peak of amu 28, CO, N_2, C_2H_4. The minor species included a peak at 44 amu believed to due to N_2O and CO_2,C_3H_6, peaks at 55 and 56 amu believed to be due to the fragmentation of C_4H_8, and trace species at 40 amu (C_3H_4) and 70 amu (C_4H_6O). Since a post-test analysis was performed, only stable species were measured and decomposition mechanisms could not be derived directly from the data. Farber[1,2] et al. conducted

mass spectrometric investigations of BAMO[1] and NMMO[2] energetic polymers. For pyrolysis of BAMO at 473 K, they found a considerable amount of H_2O and proposed that this was due to the evolution of large quantities of OH which recombined in their effusion cell to form H_2O. They also found a substantial amount of N_2 and CO but did not mention H_2. Chen[3] also tested the same BAMO/NMMO copolymer using CO_2 laser pyrolysis and a Hewlett Packard GC/MS for analysis. He observed similar major species of N_2, CO, CO_2, N_2O, C_3H_6, C_4H_8, C_2H_4, and C_4H_6O. Thus, the present results are extremely consistent with these results of Chen.

The SONY camcorder was used to film the test and no visible flame was observed. However, the picture was very quickly blocked by the vigorous evolution of a cloud of fine cream-colored particles that coated the test chamber with a fine layer of 'dust.' Farber[1] et al. noted that for decomposition of BAMO at 130-135°C, the sample turned from white to a cream color as it slowly decomposed.

3.1.2 HTPB/Zecorez

Several tests of an HTPB/Zecorez binder were performed to identify the major primary decomposition species, to investigate the reactions that occur upon ignition in air, and to study the transient response of the MPMS system. Three figures are presented in this section that are all coupled together to fulfill the desired objectives. Figure 4 gives several sections of a 0-100 amu scan of the primary decomposition species, Figure 5 displays a sequence of schlieren pictures of the ignition event, and Figure 6 presents a set of transient species profiles for the ignition event displayed in Figure 5.

The initial step in studying the HTPB/Zecorez material was to determine the primary decomposition species evolved from a pyrolyzing sample. The sample was heated by a relatively low heat flux of 50 W/cm^2 for two seconds. With this amount of energy input to the sample, no ignition occurred and no evidence of secondary reactions was observed in the schlieren movies. The microprobe sampled the gases about 2 mm above the surface after a quasi-steady state of pyrolysis was attained.

The mass spectrum from 0-100 amu was investigated with an ionization energy of 17 eV to eliminate N_2 from the results. The important sections of the spectrum are displayed in Figure 4. Major peaks were observed at 18, 28, 30, 32, 39, 42, 54, 56, 66-68, 78-80, 91, and 92 amu. Minor peaks, some of which may be due to fragments of parent hydrocarbons, were detected in the amu ranges of 16-18, 26-30, 39-44, 52-58, 65-70, 77-84, and 91-96. Pyrolysis gases from HTPB samples were analyzed in previous tests with a Hewlett Packard GC/MS and those results were used in trying to identify the peaks seen in Figure 4. With a relatively low ionization energy setting of 17 eV, little fragmentation of parent ions was expected and N_2 would not be observed because a 17 eV setting of this MPMS system was the ionization threshold above which N_2 first appeared. Burke[4] conducted high temperature oxidation studies of 1,3-butadiene and his results were also used to identify some of the peaks observed in the present tests. The major species believed to correspond to the observed

mass spectrum are CH_4, H_2O, CO, C_2H_4, CH_2O, O_2 (from the air environment), C_3H_4, C_3H_6, C_4H_6 (monomer backbone), C_4H_8, 1,3-cyclopentadiene[4] (C_5H_6), benzene (C_6H_6), cyclohexadiene (C_6H_8), and toluene (C_7H_8). The peak at 39 is believed to be due to the fragmentation (loss of an H) of either methyl acetylene or allene at amu 40 (C_3H_4). Identification of minor species was not attempted because data on cracking patterns at 17 eV of the suspected hydrocarbons was not found and the required sample gases were not available at the time of these tests.

Figure 5 presents a sequence of schlieren pictures of the ignition event for HTPB/Zecorez taken from the high-speed schlieren movies. The microprobe, protected by the probe shield, can be seen on the left side of the pictures located 8 mm above the sample surface and 6 mm off to the side of the 6 mm square sample. This test configuration was chosen to investigate both the ignition reactions and the transient response of the MPMS system. It was observed in previous tests that this material evolved a 'mushroom cloud' of pyrolyzed gases under laser heating. Ignition then occurred high in this cloud, and a flame front propagated back down to the surface. The location of the microprobe was chosen to initially sample the pyrolyzed gases in the cloud and then detect changes in these species as the flame front propagated past the probe tip.

Figure 6 displays the transient species profiles obtained during the ignition event pictured in Figure 5. It must be noted that the time scale on Figure 6 begins with the onset of laser heating and the times in Figure 5 are elapsed times from the first sign of pyrolysis gases. Thus, the zero-time on the schlieren pictures is slightly later than the actual zero-time by a length of time corresponding to inert heating of the sample before the surface reaches the critical temperature for the onset of pyrolysis. The molecular weights of the major peaks in Figure 4 were investigated along with CO_2 at 44 amu, believed to be produced by reaction of carbon-containing pyrolysis gases with oxygen in the air.

Figure 5a exhibits the initial evolution of pyrolyzed gases from the sample. The gaseous cloud first contacts the probe tip in Figure 5b. This corresponds to the abrupt rise in species profiles of molecular weights 66, 54, and 28. Ignition then occurs in the upper left center of the mushroom cloud at t=168 ms on the schlieren picture time scale. Figure 5c shows the ignition flame front propagating past the probe tip. At this time molecular weights 66 and 54 quickly decrease in peak intensity and 44 (CO_2) rapidly rises. The 28 amu peak also rapidly decreases in intensity but slightly later than 66 and 54. All the species except those at 28 and 44 amu subsequently disappear except for slight oscillations along the baseline. Figure 5d exhibits steady state burning under laser heating with the probe tip immersed in the outer flame zone.

The major primary pyrolysis species are believed to be the monomer C_4H_6, 1,3-cyclopentadiene (C_5H_6), and C_3H_4 (represented by fragment at 39 amu). These species evolve at the same time in Figure 6 and follow the same general profiles. As those species decay, the peak at 28 amu rapidly increases. This rise is caused by the oxidation of the primary hydrocarbons to form CO. Then, the 28

amu profile rapidly decreases in magnitude as the final flame develops due to oxidation of CO to CO_2.

3.2 Propellants

3.2.1 M10

One of the propellants that was tested in the checkout phase was M10. M10 is a single-base propellant consisting of 98% nitrocellulose, 1% potassium sulfate, and 1% diphenylamine. The samples used were cut into 0.64 cm high segments from a solid 0.64 cm. rod of M10. The tests were executed in nitrogen and helium environments at one atmosphere. The CO_2 Laser was used as the ignition source with heat fluxes from 40 to 200 W/cm^2.

From these tests, major products were identified with molecular weights of 18 (H_2O), 28 (N_2, CO), 30 (CH_2O, NO), and 44 (N_2O, CO_2). Other minor species detected include 27 (HCN), 46 (NO_2), and 58 ($(HCO)_2$). These species were all proposed in Fifer's review of nitrate ester propellant chemistry[5]. Figure 7 displays several species profiles as a function of laser heating time. The species profiled in this figure are each representative of a group of species that follow the same general temporal trends. The species profiles of 30 (CH_2O, NO), 46 (NC_2), and 58 ($(HCO)_2$) were quite similar in shape but of slightly different intensities. The molecular weights 18 (H_2O), 27 (HCN), and 28 (N_2, CO) also exhibit similar profiles. The species profile of 44 (N_2O, CO_2) appears to be a mix of the two previously mentioned curve shapes, possibly due to the fact that it represents two distinct species simultaneously that follow different temporal trends. The probe was initially positioned very close to the side of the sample just below the flat sample surface and the positioner was withdrawn at 1 mm/sec. Pyrolysis gases evolve and move down the side of the sample, first appearing in Figure 7 at t≈350 ms. The probe reaches the level of the sample surface at t≈675 ms where all the profiles rapidly rise. The preliminary results in Figure 7 suggest the trend proposed by numerous researchers[5] that a fizz zone exists on the sample surface where primary decomposition species (CH_2O, NO, NO_2, $(HCO)_2$)are produced which react to create secondary species (H_2O, CO and HCN) found in the dark zone.

3.2.2 BLX9

Several tests of a RDX-based propellant designated BLX9 were conducted in an attempt to resolve the gas-phase structure of chemical zones proposed by numerous investigators of nitramine-based propellants.[5-11] The major constituents of BLX9 are RDX (66%), an energetic plasticizer BTTN (23%), and GAP binder (9%). These tests were conducted primarily to check out the MPMS system spatial and temporal resolution with a propellant whose gas-phase structure is generally known. The experimental diagnostics employed included high-speed video schlieren photography, fine-wire thermocouples, and the MPMS system.

Review articles on the voluminous literature on nitramine chemistry have been published by Fifer[5], Boggs[6], and Schroeder.[7] It is well established that several chemical zones are responsible for

the observed nitramine combustion behavior. A 'fizz' zone exists directly above, and attached to, the sample surface and has a thickness of about 100 μm at a pressure of 0.05 MPa[8] and about 6 μm at P=1.0 MPa[9]. The primary decomposition species undergo reactions in this zone, producing secondary gaseous species which then enter the 'dark' zone. Temperature rises slowly as the species traverse the dark zone due to slow reactions, but the zone is basically nonreactive. The thickness of the dark zone is inversely dependent on pressure and has been measured to be about 4 mm at atmospheric pressure[10,11]. This zone terminates in a final flame zone where the secondary species react to form final stable species and temperature rises abruptly from the final dark zone temperature to the flame temperature. For neat RDX, Harris[10] gives these temperatures as about 1500 K and 2100 K, respectively.

Figure 8 displays a sequence of pictures obtained from high-speed schlieren movies of the CO_2 laser-induced ignition and combustion of a BLX9 sample. The times below the pictures are the elapsed time from the initiation of laser heating. The heat flux was 320 W/cm^2 and the heating occurred for two seconds. The environment was 91% N_2 and 9% O_2 at one atmosphere of pressure. The pictures in Figure 8 show the BLX9 sample sitting on the sample holder with its surface angled at 45° toward the 3.2 mm O.D. microprobe which is protected by a probe shield seen protruding from the top edge of the probe. The intersecting point of the crosshairs in Figures 8a and 8d designates the location of the probe sampling orifice which had a diameter of ≈60 μm. The initial sampling height was 110 μm normal to the sample surface. The appearance in these pictures that the probe tip is below the sample surface is due to the surface being slightly nonparallel to the schlieren light beam. The linear positioner was set to move the sample downward at a velocity of 4 mm/sec.

Figure 8b displays the initial evolution of pyrolyzed gases from the sample surface. These gases reach a height of slightly less than one millimeter before they ignite as seen in Figure 8c. Figure 8d displays several important features. The location of the crosshairs in Figures 8a and 8d show that the surface appears to have moved upward relative to the crosshairs. However, this phenomena is due to the existence of a zone of heavy gases attached to the sample surface which appear black because the schlieren system was adjusted to a high sensitivity setting. This zone of heavy gases is about 350 μm thick and may correspond to a laser-supported fizz zone. According to the data of Ermolin et al.[8], the fizz zone should be about 90 μm thick at one atmosphere of pressure. However, this thickness is for self-supported deflagration of RDX ignited by a nichrome wire, and it is believed that the greater thickness of the fizz zone observed here is because the deflagration is laser-supported. The thickness may also be affected by the presence of the binder.

A fluctuating reaction zone directly above the dark fizz zone can be seen in Figures 8d-8f. The primary decomposition species in the fizz zone react to form secondary species in this 'secondary reaction zone' which appears to extend to a steady state height of about 1.5 mm above the sample surface. In Figure 8e, the probe is sampling at the edge of the secondary reaction zone, and in

Figure 8f the probe has finally entered the dark zone.

Figure 9 presents the gaseous species profiles as a function of distance above the sample surface corresponding to the test displayed in Figure 8. The ionization energy was set at 25 eV. It is important to note that all species profile intensities were normalized by the intensity measured for a pure N_2 atmosphere. Thus, the chemistry suggested in Figure 9 can only be qualitatively discussed. All species profiles begin at the initiation of laser heating. Therefore, the initial changes in species profiles seen in Figure 9 are due to the transient establishment of the steady state species concentrations in the fizz zone.

The major species expected at the molecular weights investigated were NO and CH_2O at 30 amu, N_2 and CO at 28 amu, HCN (27), H_2O (18), and NO_2 (46). All species are observed in the fizz zone seen in Figure 8d. Abrupt changes in species profiles are observed at a height of about 1 mm which is about the middle of the proposed secondary reaction zone seen in Figures 8d-8f. The profiles show an abrupt decrease in NO, CH_2O, and NO_2 with a coincident increase in H_2O and HCN. These observations may correspond to the oxidation of CH_2O by NO_2 as proposed by BenReuven et al.[9] The profiles level off at about 1.4 mm which closely approximates the upper bound of the secondary reaction zone. The species profiles then remain nearly constant throughout the dark zone. Abrupt changes in species profiles occur in the luminous flame zone at a height of 4 mm. Here, the 30 amu intensity drops significantly as the 28 amu profile increases by about the same ratio. The HCN profile also drops significantly. The principal reaction occurring in this flame zone is believed to be the reduction of NO (30 amu) to N_2 (28 amu) as proposed by numerous investigators.[5-11]

Figure 10 displays a thermal profile obtained using fine-wire thermocouples. The thermocouples were constructed by welding 25 μm diameter platinum and platinum/13% rhodium wires together under a microscope as described in the first annual report for this project. This welding produces a bead of the same size as the wire diameter. The thermal profile in Figure 10 was obtained in a similar test to that which produced the results in Figures 8 and 9, but not the same test. It is presented here as further evidence of the existence of the chemical zones. High-speed videos were not taken during the thermocouple test so exact measuring heights cannot be given and the initial thermocouple position could only be closely approximated as within 0.2 mm of the sample surface. The temperature initially rose to 815 K. Fetherolf et al.[12] measured a surface temperature of 720 K for BLX9, so it is believed that the initial temperature measured here corresponds to the beginning of the fizz zone directly above the sample surface. The temperature then slowly increased as the sample burned away and was withdrawn by the linear positioner. At a temperature of about 1100 K, the temperature rose abruptly to 1400 K. Estimates of the thermocouple position based upon surface regression rate and positioner speed show that the leveling off of the thermal profile at 1400 K occurs at a height of approximately 1.2 mm, which closely corresponds to the end of the secondary reaction zone. Harris[10] measured a dark zone temperature of 1500 K for neat RDX, and it

is expected that the dark zone temperature of the BLX9 propellant would be lower due to the influence of the binder decomposition species.

4.0 SUMMARY

The second year of the program has produced significant improvements in the MPMS system including lowering the spatiai resolution to nearly 100μm. The preliminary results obtained on all of the materials tested are consistent with the results of previous investigators. Furthermore, the BLX-9 species results show the various zones characteristic of nitramine propellants and coincide extremely well with the thermal profiles from microthermocouple tests of the same material. Thus, the MPMS system is fully operational, although improvements will be made whenever possible. Tests with pure nitramines will be the focus of the work of the third year.

REFERENCES

1. Farber, M., Harris, S. P., Srivastava, R. D., "Mass Spectrometric Kinetic Studies on Several Azido Polymers," *Combustion and Flame*, Vol. 55, 1984, pp. 203-211.
2. Farber, M., Harris, S. P., Srivastava, R. D., "Mass Spectrometric Investigation of the Thermal Decomposition of Several Propellant and Explosive Ingredients," Final Report, Contract N00014-80-C-0711, Space Sciences, Inc., Monrovia, CA, February 1986.
3. Chen, D. M., "Pyrolysis, Ignition, and Combustion of Solid Fuels for Ramjet Applications," Ph. D. Thesis, The Pennsylvania State University, Dept. of Fuel Science, Aug. 1988.
4. Burke, E.,"High Temperature Pyrolysis of 1,3 Butadiene ...," Masters of Science Thesis, Princeton University, Dept. of
5. Fifer, R. A., "Chemistry of Nitrate Ester and Nitramine Propellants," Chapter 4, Progress in Astronautics and Aeronautics: Fundamentals of Solid Propellant Combustion, edited by K. K. Kuo and M. Summerfield, AIAA, Vol. 90, 1984.
6. Boggs, T. L., "The Thermal Behavior of Cyclotrimethylene-trinitramine (RDX) and Cyclotetramethylenetetranitramine (HMX)," Chapter 3, Progress in Astronautics and Aeronautics: Fundamentals of Solid Propellant Combustion, edited by K. K. Kuo and M. Summerfield, AIAA, Vol. 90, 1984.
7. Schroeder, M. A., "Critical Analysis of Nitramine Decomposition Data: Product Distributions from HMX and RDX Decomposition," Proceedings of the 18th JANNAF Combustion Meeting, Pasadena, CA, October 1981, CPIA Publ. No. 347, Vol. II, pp. 395-413.
8. Ermolin, N. E., Korobeinichev, O. P., Kuibida, L. V., Fomin, V. M., "Study of the Kinetics and Mechanism of Chemical Reactions in Hexogen Flames," translated from *Fizika Goreniya i Vzryva*, Vol. 22, No.5, Sept.-Oct. 1986, pp. 54-64.
9. BenReuven, M., Caveny, L. H., Vichnevetsky, R. J., Summerfield, M., "Flame Zone and Sub-surface Reaction Model for Deflagrating RDX, " Proceedings of the 16th Symposium (International) on Combustion, The Combustion Institute, Pittsburgh, PA, 1982, pp. 1223-1233.
10. Harris, L. E., "CARS Spectroscopy of the Reaction Zone of Methane-Nitrous Oxide and RDX Propellant Flames," Report ARAED-TR-85007, January 1986, U. S. Army Armament Research and Development Center, Dover, NJ.
11. Parr, T., Hanson-Parr, D., "Species and Temperature Profiles in Ignition and Deflagration of HMX," Paper 87-8, Spring Meeting, Western States Section, The Combustion Institute, April 6-7, 1987, Provo, Utah.
12. Fetherolf, B. L., Kim, J. U., Litzinger, T. A., Kuo. K. K., "CO_2 Laser-induced Pyrolysis and Ignition Processes of Nitramine Composite Propellants," presented as a poster paper at The 22nd

Symposium (International) on Combustion, The Univ. of Washington, Seattle, WA, Aug. 14-19, 1988.

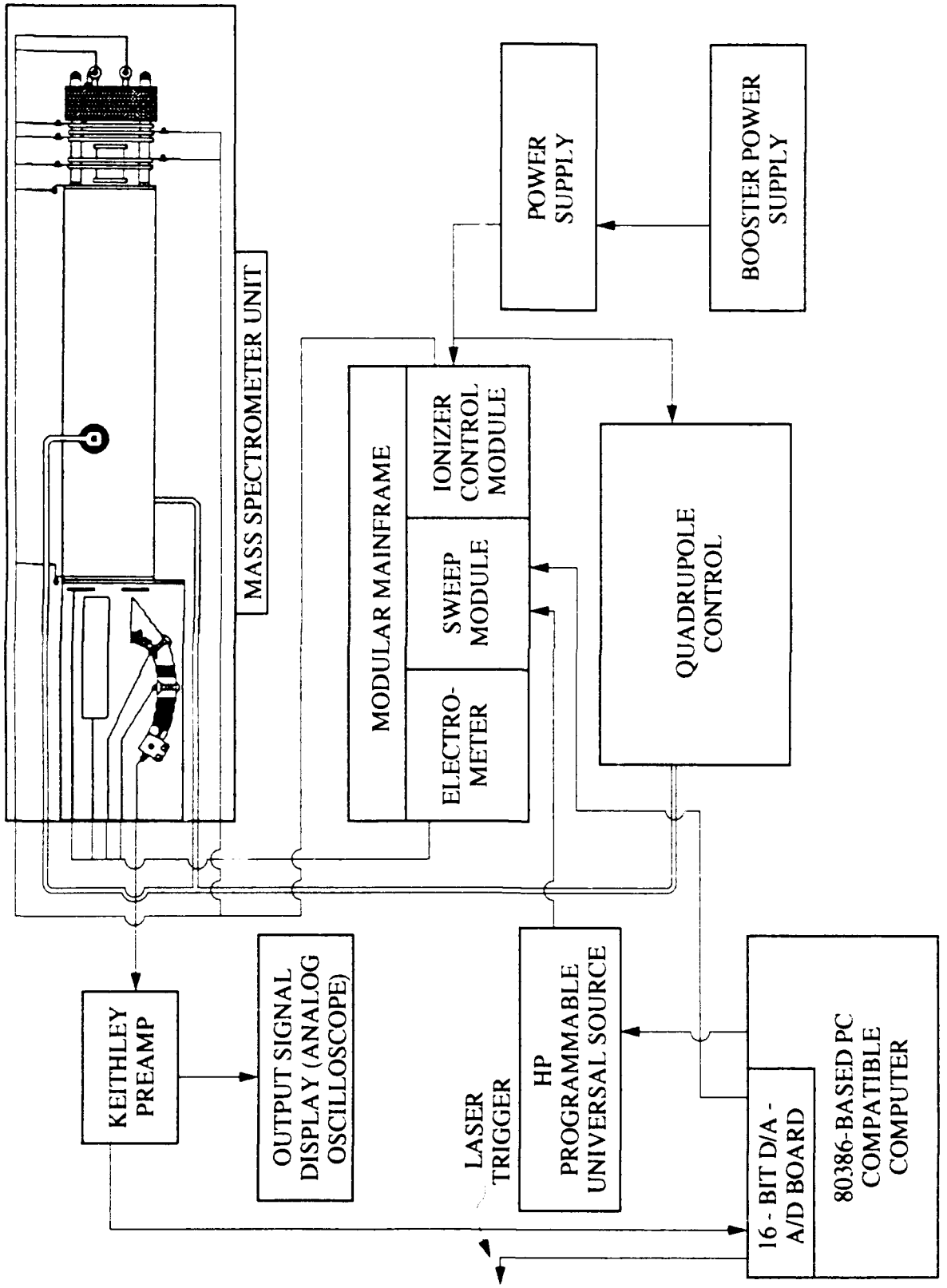

Figure 1. Block diagram of modified quadrupole mass spectrometer electronic control system

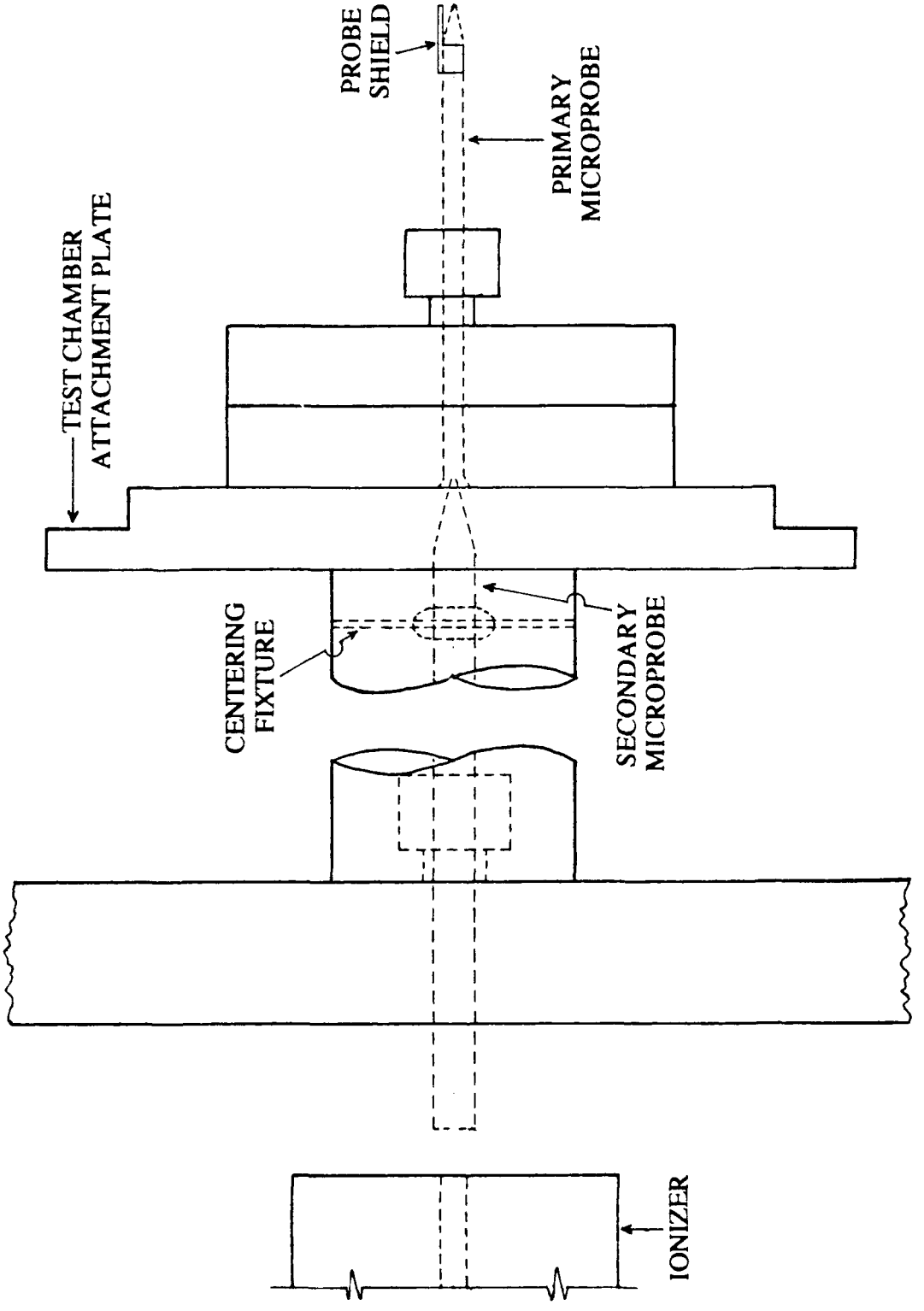

Figure 2. Schematic diagram of gas sampling system

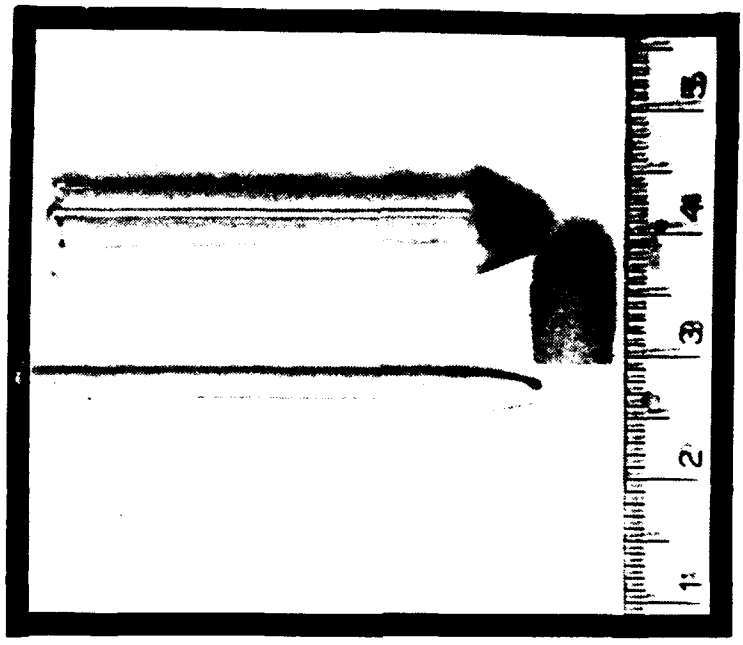

Figure 3. Photograph of microprobes with BLX9 sample (ruler scale is 1 mm per small division)

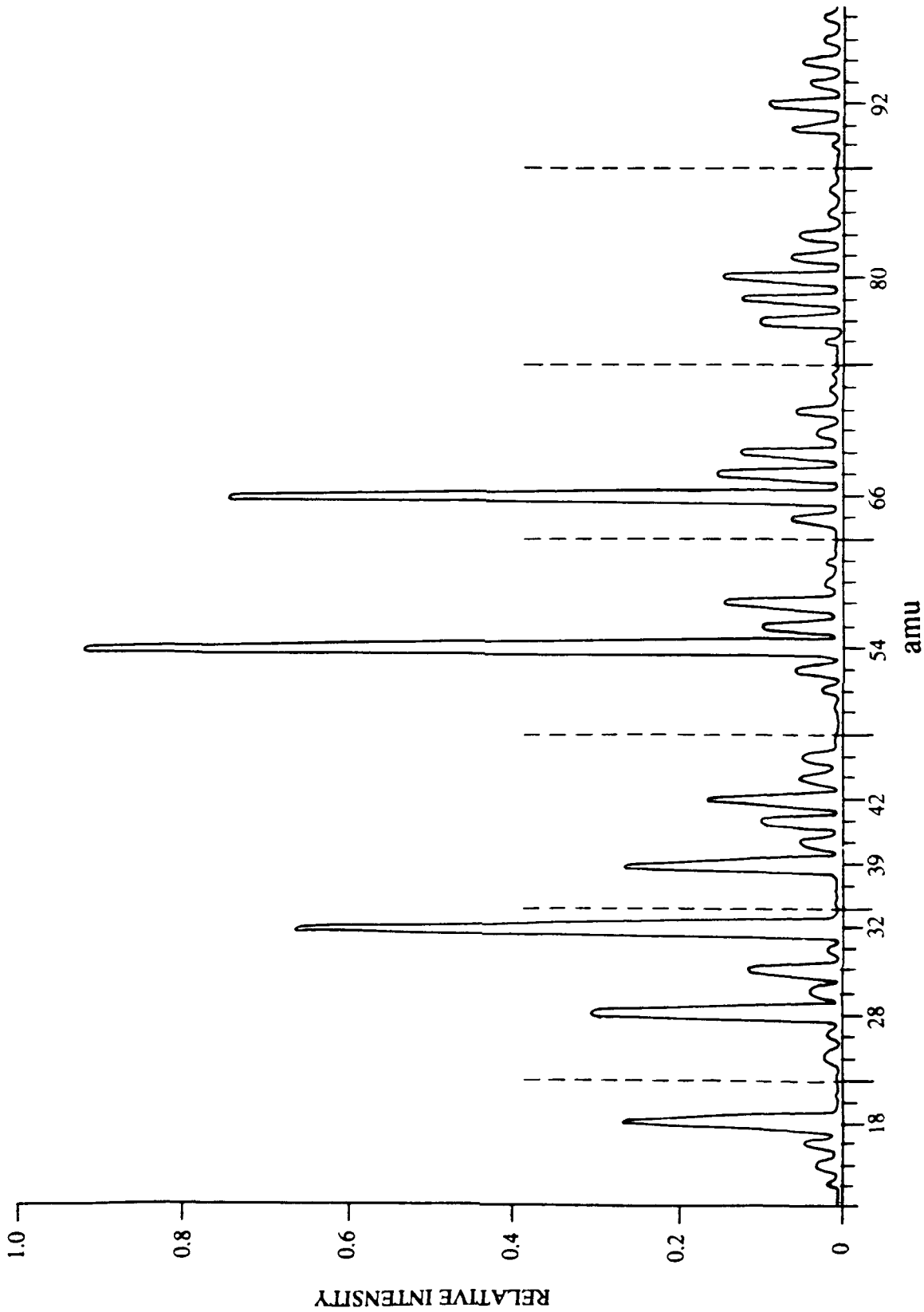

Figure 4. Sections of mass spectrum from 0-100 amu for the decomposition products of HTPB/Zecorez ($q'' = 100$ W/cm^2, P = 1 atm of air)

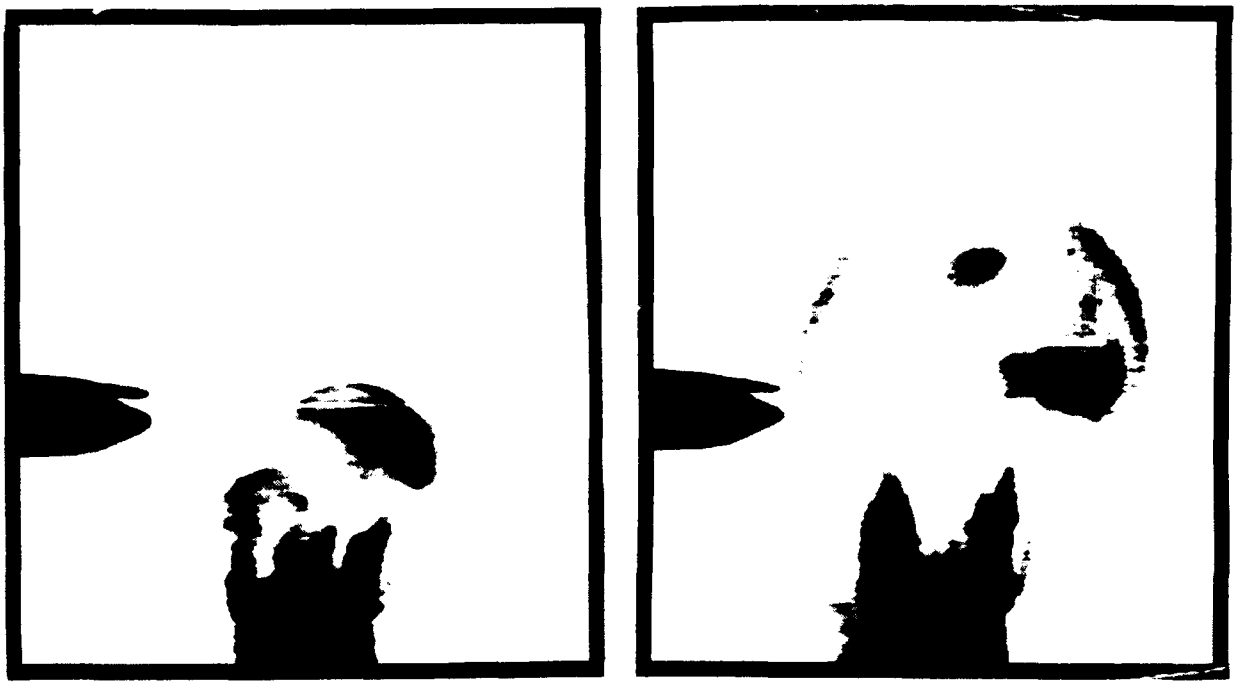

(a) t = 106 ms (b) t = 140 ms

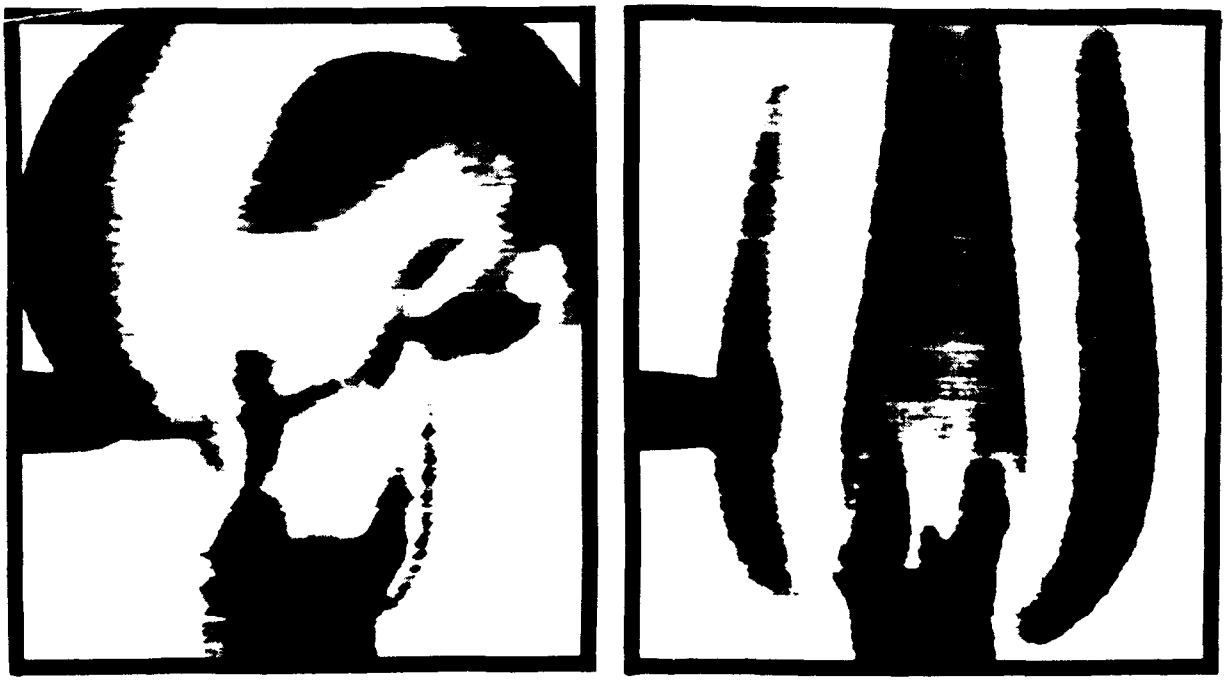

(c) t = 172 ms (d) t = 267 ms

Figure 5. Sequence of schlieren pictures for the laser-induced ignition of HTPB/Zecorez
($q'' = 100$ W/cm^2, P = 1 atm of air)

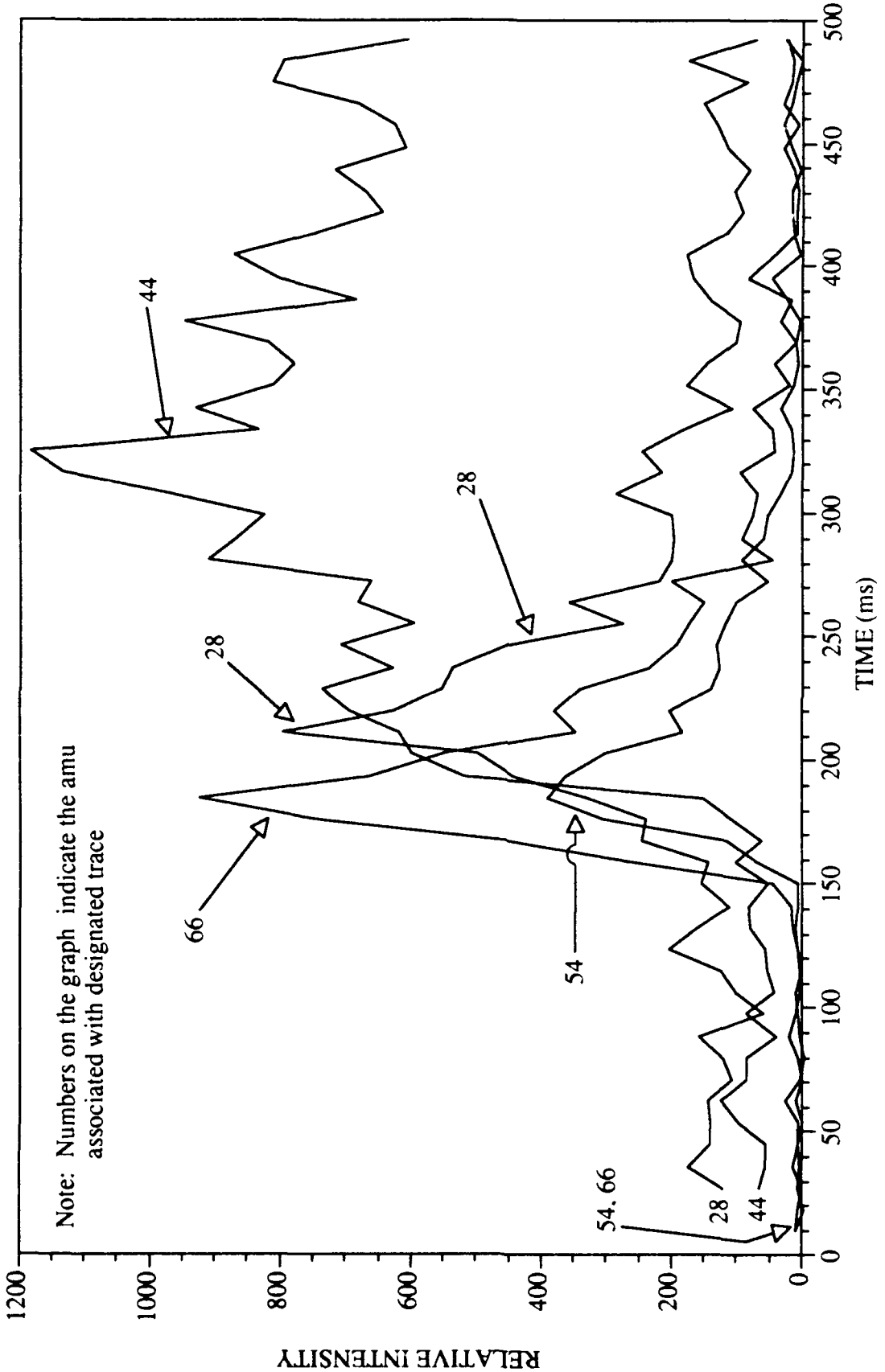

Figure 6. Gaseous species profiles as a function of laser heating time for HTPB/Zecorez sample ($q'' = 100$ W/cm^2, P = 1 atm of air)

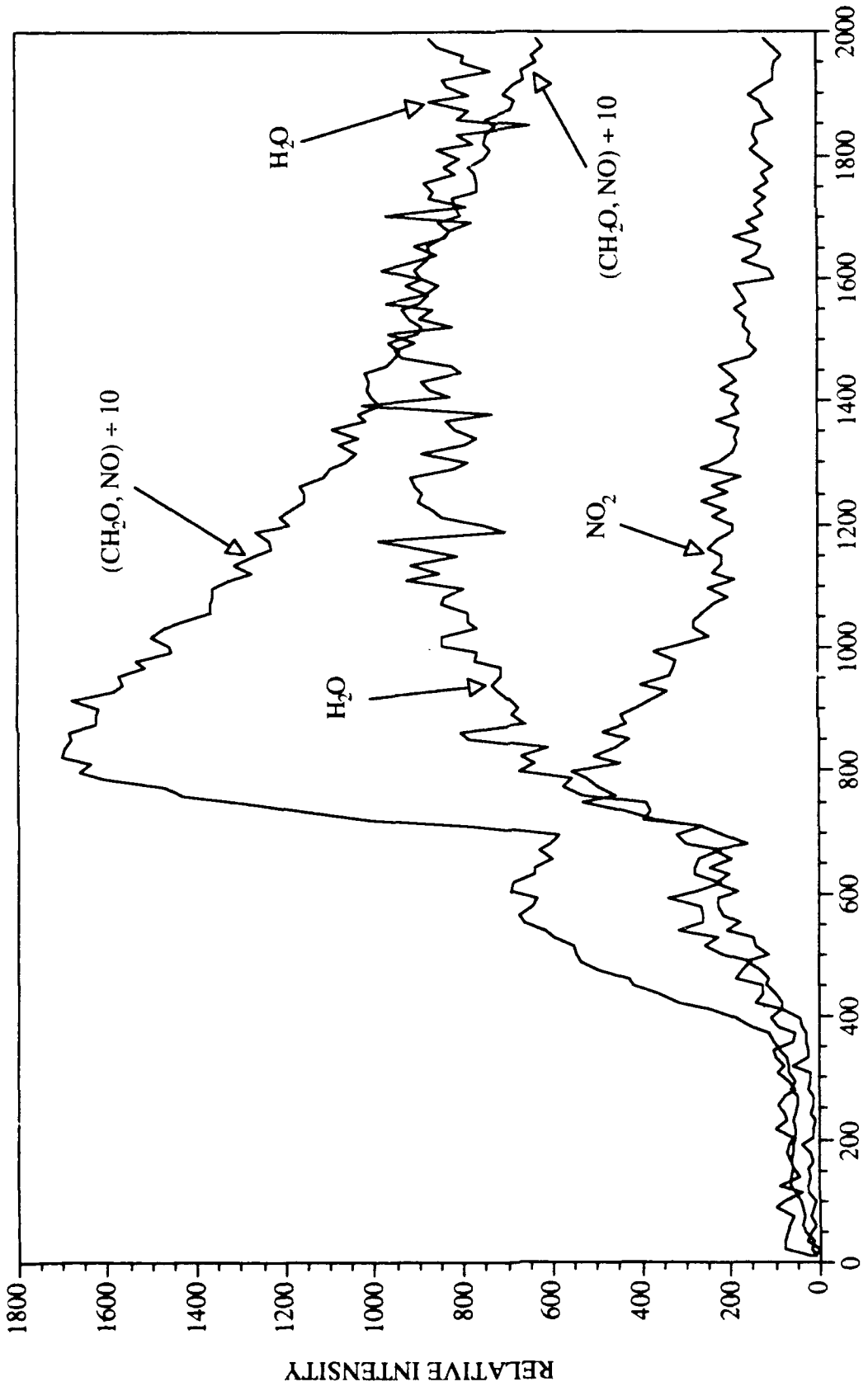

Figure 7. Gaseous species profiles as a function of laser heating time for M10 sample ($q'' = 100$ W/cm^2, P = 1 atm of N_2)

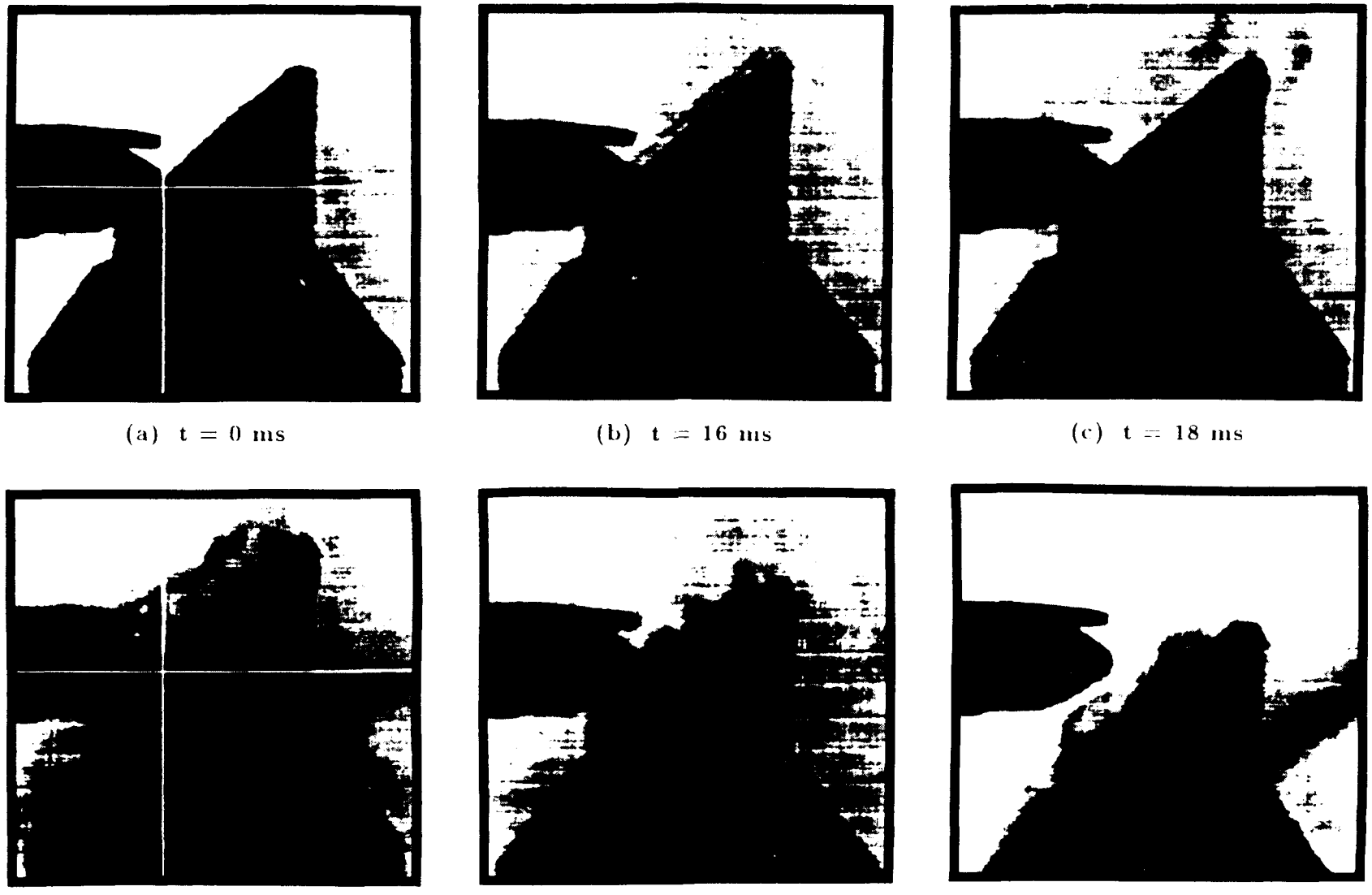

(a) t = 0 ms (b) t = 16 ms (c) t = 18 ms

(d) t = 37 ms (e) t = 296 ms (f) t = 519 ms

Figure 8. Sequence of schlieren pictures of the laser-induced ignition and deflagration of BLX9 ($q'' = 320$ W/cm^2, P = 1 atm of 91% N_2, 9% O_2)

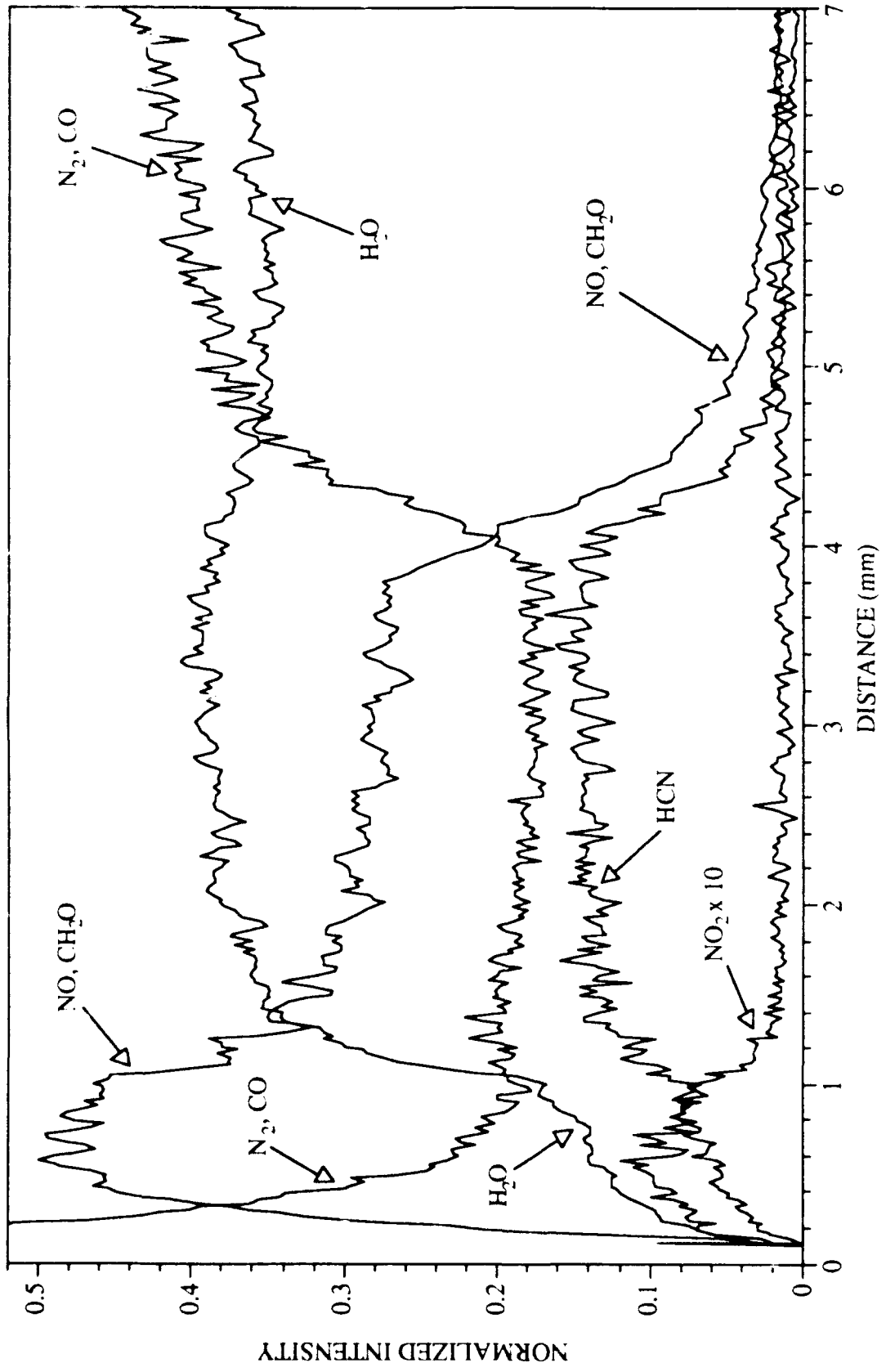

Figure 9. Gaseous Species Profiles as a function of distance above burning RDX-based propellant ($q'' = 320$ W/cm^2, P = 1 atm of N_2)

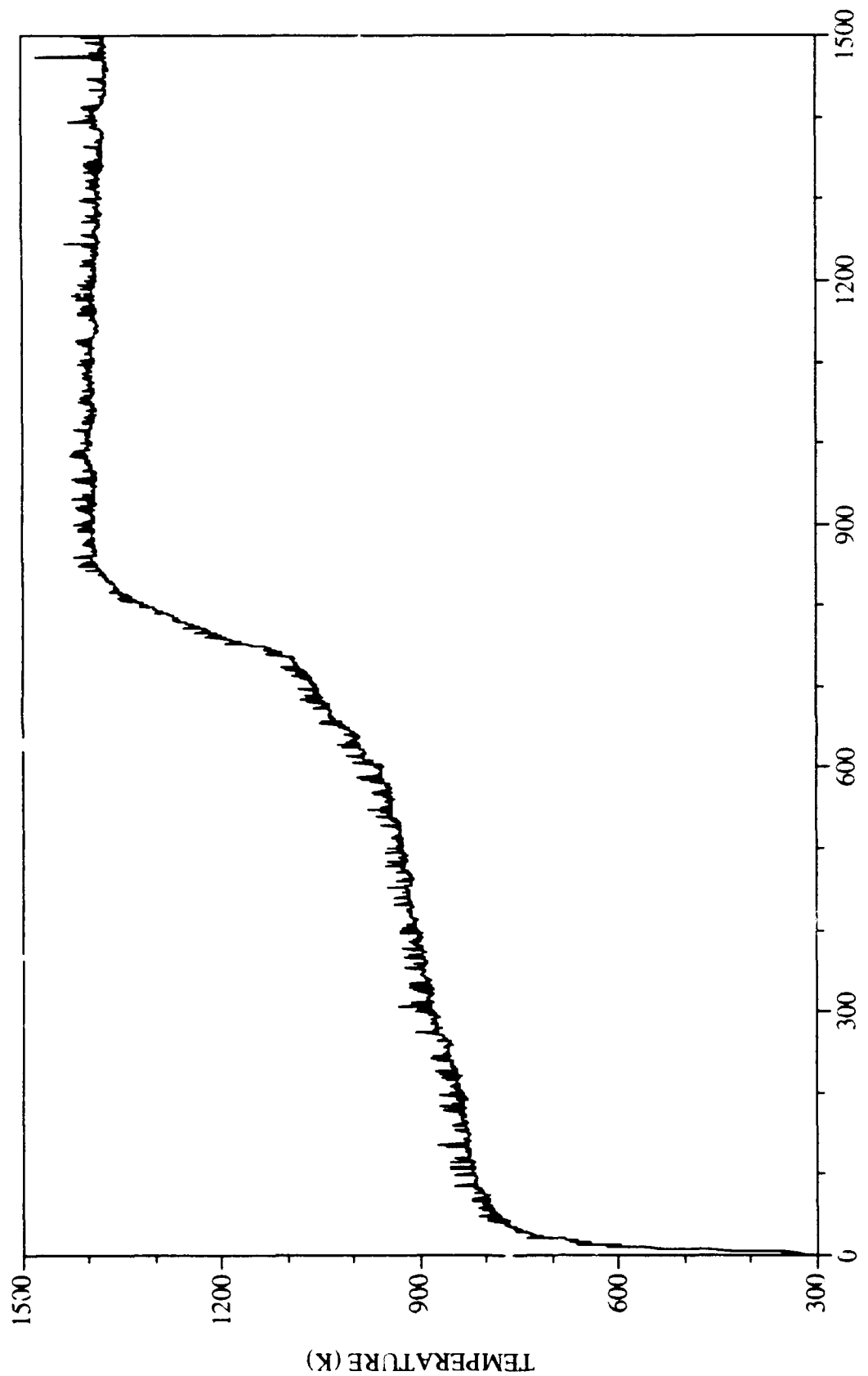

Figure 10. Temperature trace as a function of laser heating time for BLX9 sample ($q'' = 460$ W/cm^2, P = 1 atm of He)